# Two-glassy-phase bulk metallic glass with remarkable plasticity

X. H. Du
*Institute of Materials Science and Engineering, National Sun Yat-Sen University, Kaohsiung, Taiwan 804, Republic of China and Department of Materials Engineering, Shenyang Institute of Aeronautical Engineering, Shenyang, 110034, People's Republic of China*

J. C. Huang,[a] K. C. Hsieh, Y. H. Lai, and H. M. Chen
*Institute of Materials Science and Engineering, Center for Nanoscience and Nanotechnology, National Sun Yat-Sen University, Kaohsiung, Taiwan 804, Republic of China*

J. S. C. Jang
*Department Materials Science and Engineering, I-Shou University, Kaohsiung, Taiwan 840, Republic of China*

P. K. Liaw
*Department Materials Science and Engineering, University of Tennessee, Knoxville, Tennessee 37996, USA*

(Received 19 July 2007; accepted 7 September 2007; published online 25 September 2007)

Using the computational-thermodynamic approach, the potential compositions of Zr–Cu–Ni–Al alloy system exhibiting the two-liquid miscibility phase equilibrium in the liquid temperature region have been identified. The resulting Zr base bulk metallic glasses show a microstructure of two microscaled glassy phases. The glass possesses a remarkable macroscopic plastic strain of 30% at room temperature. The gain of mechanical properties is attributed to the unique glassy structure correlated with the chemical inhomogeneity on the micron scale, the hard phases surrounded by the soft phases, leading extensive shear-band formation, interactions, and multiplication. © *2007 American Institute of Physics*. [DOI: 10.1063/1.2790380]

One exciting benefit of preparing bulk metallic glasses (BMGs) is a tremendous gain in high yield strength. However, even for some tougher zirconium or palladium based metallic glasses, their applicability is limited by the lack of plasticity resulting from shear localization and work softening.[1] To overcome this limited plasticity, two ways have been exploited: one is intrinsic toughening by increasing Poisson's ratio,[2,3] and the other is extrinsic toughening by developing a composite microstructure within the glassy matrix.[4–7] In particular, the discovery of the superplastic BMGs at room temperature sheds light that BMGs seem to have the potential to exhibit remarkable plasticity if some unique structures, e.g., a two-glassy-phase structure, are available.[2,7]

In intermetallic alloys and ceramics, we can improve the mechanical properties by forming a duplex or multiphase microstructure which can provide effective obstacles for the propagating microcracks.[8,9] Following these ideas, the development of a two-glassy-phase microstructure is expected to be of potential interest in terms of the ductility improvement of BMGs. The early efforts to obtain two-glassy-phase BMGs usually involve the addition of alloying elements with a positive enthalpy of mixing into the master alloy systems and, thus, inevitably make the resultant BMGs to inherit inferior glass formation ability (GFA).[10]

To overcome the dilemma, it is necessary to prepare dual-glassy-phase BMGs with high GFA. We note that the Zr–Cu–Ni–Al alloy system is a good candidate for this investigation, since it shows a high GFA and includes an atomic pair with a positive enthalpy of mixing between Ni and Cu elements.[11] However, how to pinpoint the composition of an alloy exhibiting phase separation appears to be a scientific challenge.

Yan *et al.* have explored a computational-thermodynamic approach to identify the potential compositions of Zr–Ti–Ni–Cu alloys exhibiting low-lying liquidus surfaces that favor the glass formation[12] in reasonable agreement with those determined experimentally by Lin and Johnson.[13] A salient feature of this approach is that the thermodynamic models of the phases implicitly incorporate the multiple chemical and topological interactions among component elements through the enthalpy and entropy terms. Besides, we need to employ a "thermodynamic description" concept on the basis of the description of a multicomponent system obtained by the CALPHAD approach.[14] For the quaternary system, there are six constituent binaries and four constituent ternaries. Using the quaternary thermodynamic description obtained and the commercial software PANDAT,[15] the isotherms and isopleths can be calculated.

For the quaternary system, the complete isotherm is a tetragonal volume under a constant pressure, and then, a two-dimensional section can be obtained from cutting with constant Al content. This will provide the information for the selection of alloy compositions. In this study, the selected *X* alloy within the two immiscible liquid phase regions ($L1$ and $L2$) can be found in the 1050 °C isothermal section, from which the isopleth cut for $Al_5Ni_{40}Zr_{55}$ and $Al_5Cu_{25}Zr_{70}$ composition regions is determined, as shown in Fig. 1. According to the diagram, the *X* alloy with the optimum composition of $Zr_{63.8}Ni_{16.2}Cu_{15}Al_5$ is located in the two-liquid-phase region, and the compositions of the two calculated liquid phases are Ni-rich $Zr_{68.4}Ni_{23.9}Cu_{6.6}Al_{1.1}$ and Cu-rich $Zr_{61.7}Ni_{12.8}Cu_{18.8}Al_{6.7}$, respectively.

Based on the selected optimum composition within the two liquid-phase region, $Zr_{63.8}Ni_{16.2}Cu_{15}Al_5$, cylindrical ingots of the Zr base BMG, 2 mm in diameter, were prepared

[a]Author to whom correspondence should be addressed; electronic mail: jacobc@mail.nsysu.edu.tw

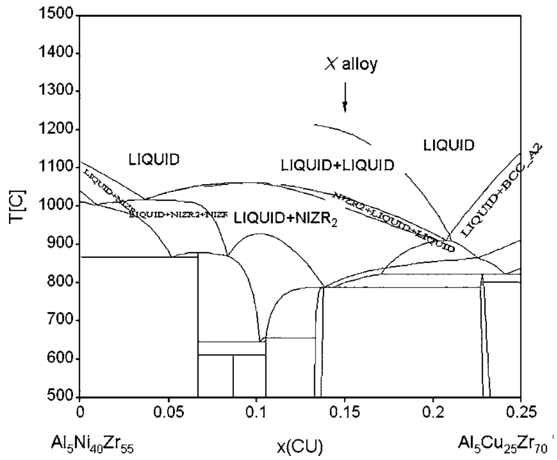


FIG. 1. The simulated phase diagram for the composition cut between $Al_5Ni_{40}Zr_{55}$ and $Al_5Cu_{25}Zr_{70}$.

by arc melting the pure elements under a purified Ar atmosphere and *in situ* suction casting in a copper mold. The rod specimens with an aspect ratio of 2:1 were tested in compression under an initial strain rate of $2\times10^{-4}$ s$^{-1}$ at room temperature.

Figure 2(a) shows the as-cast structure under the scanning electron microscope (SEM), which is macroscopically homogenous without observable crystals and other cast defects. The x-ray diffraction (XRD) curve of the as-cast ingot is inserted in Fig. 2(a). The diffuse hump in the XRD curve, coupled with the clear glass transitions and sharp crystallization events in the differential scanning calorimetry curve, confirms the glassy nature of the BMGs. $T_g$, $T_x$, $\Delta T_x$, and $T_l$ of the current Zr BMG are 647, 745, 98, and 1178 K, respectively. The GFA parameters such as $\gamma[=T_x/(T_g+T_l)]$ (Ref. 16) and $\gamma_m[=(2T_x-T_g)/T_l]$ (Ref. 17) are 0.41 and 0.72, respectively. The corresponding critical cooling rate to produce glass phase is around 1 K/s.[17] All of these results prove that the alloy has good glass forming ability. It is interesting that the transmission electron microscopy (TEM) bright-field images and the corresponding selected area-diffraction pattern of sites I and II [Figs. 2(b) and 2(c)] clearly show the presence of two different glassy phases with brighter and darker contrasts for the Zr BMG. The global second glassy phase having a darker contrast is embedded in the lighter glassy matrix. The high resolution electron-microscopy (HREM) image taken at the interface III [Fig. 2(d)] shows a homogenous maze pattern, indicating that the two glassy phases with different compositions combine perfectly.

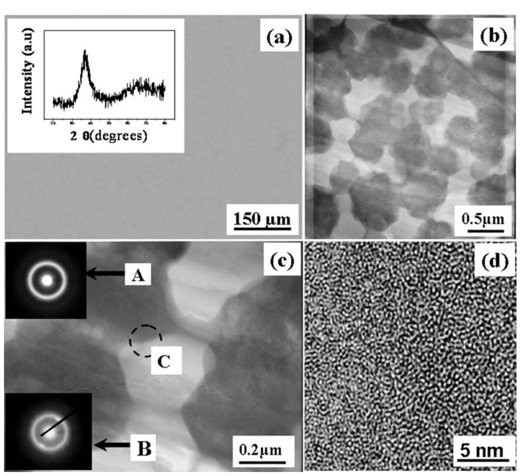


FIG. 2. Microstructures of the 2 mm diameter Zr base BMG rod: (a) SEM image of the etched as-cast microstructure with the inserted XRD pattern, [(b) and (c)] TEM bright-field image, and (d) HREM image of the interface marked by III in (c).

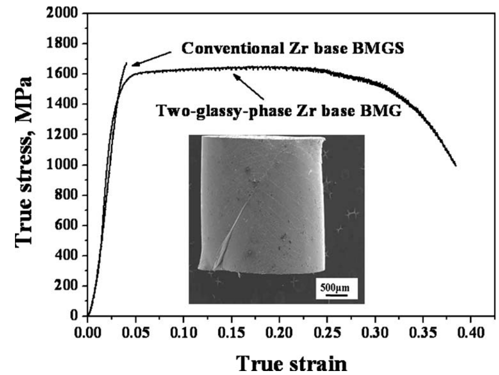


FIG. 3. Room-temperature stress-strain curve for as-cast 2 mm diameter cylinders. The inset shows the deformed sample.

The TEM/energy dispersive spectroscopy (EDS) composition analysis of the two phases gives a Ni-rich composition of $Zr_{68.5}Cu_{8.1}Ni_{21.3}Al_{2.1}$ for the darker phase while a Cu-rich composition of $Zr_{62.4}Cu_{16.7}Ni_{14.6}Al_{6.3}$ for the lighter matrix. The characteristic length scale for the glassy phases with darker contrast is 0.5–1 $\mu$m, which differs from the much finer scale for the solid-state spinodal decomposition. It is likely that the two glassy phases are directly formed from the two separated liquid phases. The results support the validity of the prediction based on the computational-thermodynamic approach.

Figure 3 shows the room-temperature true stress-strain curve for as-cast 2 mm diameter cylinders under compression loaded at a strain rate of $2\times10^{-4}$ s$^{-1}$. Under quasistatic loading, the material exhibits yield stress $\sigma_y=1.60$ GPa. On further deformation, plastic deformation at a roughly constant flow stress appears. The two-glassy-phase BMG exhibits its remarkable plasticity with the compressive true strain up to about 30%. After that, flow instability becomes dominant, meaning that shear-band localization initiates, as shown in the inserted image of the deformed specimen. The overall failure true strain exceeds 35%. However, it is noted that once the strain exceeded 30%, the major shear band would touch the upper or lower test platen, thus the further straining does not have any physical meaning.

The specimen and fracture surfaces after deformation are investigated by SEM, as shown in Fig. 4. Figure 4(a) presents the image of the strong interaction of shear bands with some phases with light contrast. The SEM/EDS analyses prove that they are the second glassy clusters on the deformed surface. The shear bands propagate preferentially through many second glassy clusters, occasionally initiate or terminate within the clusters. However, the shear bands are highly branched and their movement is rather wavy in nature. This trend suggests that the dispersed second glassy phase clusters act as a network in the glassy matrix, thus separate and restrict the highly localized shear banding to isolated regions, avoiding catastrophic shearing off through the whole sample. The fracture surface analysis [Fig. 4(b)] reveals two distinct morphologies: (i) veinlike pattern and (ii) highly rough regions. Figure 4(c) is a part within the highly rough regions, where the shear bands can be clearly observed. According to the state of shear bands, the fracture surface can be divided into the I and II regions, as shown in

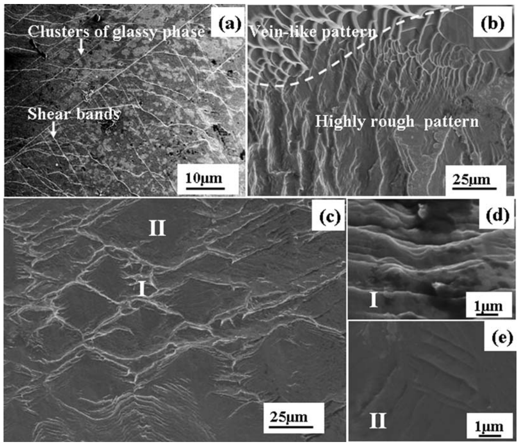


FIG. 4. Observations of the sample and fracture surface after deformation: (a) SEM image of the specimen surface, (b) SEM image of fracture surface, (c) shear-bands pattern on the fracture surface, (d) shear banding in region I, and (e) shear banding in region II.

Fig. 4(c). By SEM/EDS analyses, the compositions of regions I and II are different, and resemble the compositions measured by TEM/EDS for the glassy phases with lighter and darker contrasts, respectively. The size of second glassy phases observed by SEM is obviously much larger than the TEM observations, this is reasonable since the SEM reveals the "congregated" or the clusters of the second glassy phases. The limited length of the abundant shear bands surrounding region B indicates the strong interaction between shear bands and second glassy phases. Figures 4(d) and 4(e) show the shear bands morphology in regions I and II, respectively, at a higher magnification. The shear bands in region I are wavy and branched, and the periodicity of the wave is about 0.5–1.5 $\mu$m [Fig. 4(d)]. The consistency between the wave periodicity of shear bands (0.5–2 $\mu$m) and the size scale of second glassy phase (around 0.5–1 $\mu$m) suggests that there exists strong interaction between shear bands and second glassy phases. Most interestingly, interaction of less wary shear bands is also observed in region II of the fracture surface, as illustrated in Fig. 4(e). This trend indicates a homogeneous nucleation and distribution of shear bands throughout the BMG to accommodate the applied strain rather than the accumulation of damage at some particular shear bands, as seen in monolithic BMGs.[18]

The HREM observations did not reveal nanocrystals even in heavily deformed flakes. This trend indicates that the remarkable plasticity is not a result of the stress-induced nanocrystallization found in other BMGs.[19]

We know that a direct result of the phase separation is the emergence of the regions with different chemical compositions, different coordinate numbers, and different closest neighbors. This will cause the inhomogeneous distribution of hardness (and modulus) in the BMG. In this case, the softer Cu-rich glassy phase in the two-phase BMG is the glassy matrix with a brighter contrast, and the local hardness measured by nanoindentation for the bright phases is $5.22 \pm 0.04$ GPa, which is softer than that of the dark phases ($6.17 \pm 0.04$ GPa). They might possess different critical shear stresses (CSSs) for activating shear bands.[20] The softer glassy matrix should have more open free volumes, thus exhibiting higher Poisson's ratio $\nu$,[21] which will benefit the initiation of shear bands due to the lower CSS. When yielding occurs, the relatively soft glassy phase, i.e., the matrix in this case, will become preferentially the shear-transformation zones, serving as the nucleation sites for the shear bands. Consequently, abundant shear bands can be observed in the soft matrix regions, as shown in Fig. 4(c).

On the other hand, there exists a large amount of well bonded interfaces between the two glassy phases in the current BMG. As a result, the shear-band propagation would be impeded by the second glassy phase clusters with a higher CSS, and this trend will alter the propagation directions and assist shear-band multiplication, resulting in the wavelike appearance of shear bands [Fig. 4(d)], as also observed by Xing *et al.*[6] So the micron-scale inhomogeneity resulted from phase separation would possess the ability to hinder the propagation of shear bands, resulting in multiple shear banding.

The present work shows that, by the two-liquid phase separating based on the thermodynamic prediction, a good GFA Zr base BMG can be achieved. The Zr base BMG shows remarkable plasticity through the formation of a two-glassy microstructure composed of hard regions surrounded by soft regions, which enables easy and homogeneous nucleation of the shear bands and continuous multiplication during deformation. The present results for the two-phase BMG are promising and demonstrate the possibility of designing other ductile bulk metallic glasses by the thermodynamic prediction.

This work is sponsored by National Science Council of Taiwan, ROC (No. NSC 95-2218-E-110-006). P.K.L. appreciated the support of the National Science Foundation International Materials Institutes (IMI) Program (DMR-0231320) with Dr. C. Huber as the Program Director.

[1]W. H. Wang, C. Dong, and C. H. Shek, Mater. Sci. Eng., R. **44**, 45 (2004).
[2]Y. H. Liu, G. Wang, R. J. Wang, D. Q. Zhao, M. X. Pan, and W. H. Wang, Science **315**, 1385 (2007).
[3]J. Schroers and W. L. Johnson, Phys. Rev. Lett. **93**, 255506 (2004).
[4]C. C. Hays, C. P. Kim, and W. L. Johnson, Phys. Rev. Lett. **84**, 2901 (2000).
[5]K. F. Yao and C. Q. Zhang, Appl. Phys. Lett. **90**, 061901 (2007).
[6]L. Q. Xing, Y. Li, K. T. Ramesh, J. Li, and T. C. Hufnagel, Phys. Rev. B **64**, 180201 (2001).
[7]K. F. Yao, F. Ruan, Y. Q. Yang, and N. Chen, Appl. Phys. Lett. **88**, 122106 (2006).
[8]A. G. Evans, J. Am. Ceram. Soc. **73**, 187 (1990).
[9]R. W. Cahn, D. R. F. West, D. J. Dunstan, M. McLean, J. W. Martin, and D. Morris, Philos. Trans. R. Soc. London, Ser. A **351**, 497 (1995).
[10]B. J. Park, H. J. Chang, W. T. Kim, and D. H. Kim, Appl. Phys. Lett. **85**, 6353 (2004).
[11]T. Zhang, A. Inoue, and T. Masumoto, Mater. Trans., JIM **32**, 1005 (1991).
[12]X. Y. Yan, Y. A. Chang, Y. Yang, F. Y. Xie, S. L. Chen, F. Zhang, S. Daniel, and M. H. He, Intermetallics **9**, 535 (2001).
[13]X. H. Lin and W. L. Johnson, J. Appl. Phys. **78**, 6514 (1995).
[14]Y. A. Chang, S. Chen, F. Zhang, X. Yan, F. Xie, R. Schmid-Fetzer, and W. A. Oates, Prog. Mater. Sci. **49**, 313 (2004).
[15]PANDAT, 6.0-Phase Diagram Calculation Software for Multicomponent Systems, CompuTherm LLC, 437 S. Yellowstone Dr., Suite 217, Madison, WI 53719, USA.
[16]Z. P. Lu and C. T. Liu, Phys. Rev. Lett. **91**, 115505 (2004).
[17]X. H. Du, J. C. Huang, C. T. Liu, and Z. P. Lu, J. Appl. Phys. **101**, 086108 (2007).
[18]C. A. Schuh and T. G. Nieh, Acta Mater. **51**, 87 (2003).
[19]M. W. Chen, A. Inoue, W. Zhang, and T. Sakurai, Phys. Rev. Lett. **96**, 245502 (2006).
[20]B. P. Kanungo, S. C. Glade, P. A. Kumar, and K. M. Flores, Intermetallics **12**, 1073 (2004).
[21]T. Ichitsubo, Phys. Rev. Lett. **95**, 245501 (2005).